

## IV-D Electronic and Magnetic Properties of $\pi$ -Electron-Based Molecular Systems

$\pi$ -electrons are an interesting building block in architecting functionalized electronic and magnetic molecular systems. We have focused on nano-sized graphite and TTF-based organic charge transfer complexes, in which  $\pi$ -electrons play an important role, in developing new types of molecular electronic systems. In nanographene, single layer nanographite, which is defined as flat open  $\pi$ -electron system have edges and contrasted to closed  $\pi$ -electron systems of fullerenes and carbon nanotubes, non-bonding  $\pi$ -electronic state appearing around the Fermi level generates unconventional nanomagnetism. We have found an interesting electronic wave interference effect in finite-sized graphite with distortion-network structures and anisotropy of the Raman spectra of nanographite ribbons. A combination of TTF-based  $\pi$ -electron donor and counteranion having localized spins is a useful way in producing molecular magnetic conductors, which are expected to have properties different from traditional metal magnets featured with  $s$ - $d$  interaction. Under this scheme, we have developed a new class of TTF-based organic magnetic conductors. The interaction between the conducting  $\pi$ -electrons of donors and the localized  $d$ -electrons of magnetic anions are found to show interesting interplay between magnetism and electron transport.

### IV-D-1 Weak-Ferromagnetism in Molecular Magnets Based on Transition Metal Complexes of Crown Thioether

NISHIJO, Junichi<sup>1</sup>; NIYAZAKI, Akira<sup>1</sup>; ENOKI, Toshiaki<sup>2</sup>

(<sup>1</sup>Tokyo Inst. Tech.; <sup>2</sup>IMS and Tokyo Inst. Tech.)

[*Polyhedron* **22**, 1755–1758 (2003)]

A new class of molecular based magnets  $M(9S3)_2$  [ $Ni(bdt)_2$ ]<sub>2</sub> ( $M = Ni, Co$ ) consisting of transition metal complex of crown thioether show weak-ferromagnetic transitions at  $T_N = 6.2$  and  $2.6$  K for  $M = Ni$  and  $Co$ , respectively, accompanied by remanent magnetizations  $0.2\mu_B$  and  $0.01\mu_B$  with coercive forces  $200$  and  $10$  Oe.  $M(9S3)_2^{2+}$  cations ( $S = 1$  and  $1/2$  for  $M = Ni$  and  $Co$ , respectively), and a half of  $Ni(bdt)_2^-$  ( $S = 1/2$ ) anions form alternate antiferromagnetic (AF) chains (#1), while the other half of  $Ni(bdt)_2^-$  anions form uniform AF chains (#2). These two type of chains are connected to each other by two weak AF interactions; interaction between  $Ni(bdt)_2^-$  in #1 and  $Ni(bdt)_2^-$  in #2, and interaction between  $M(9S3)_2^{2+}$  in #1 and  $Ni(bdt)_2^-$  in the adjacent chain #1. A competition between these two AF interactions causes canted spin configuration, giving rise to weak-ferromagnetism.

### IV-D-2 New Bulk Weak Ferromagnet in Ferrimagnetic Chains of Molecular Material Based on DTDH-TTP and Paramagnetic Thiocyanato Complex Anion: (DTDH-TTP)[Cr(isoq)<sub>2</sub>(NCS)<sub>4</sub>]

SETIFI, Fatima<sup>1</sup>; OUAHAB, Lahcène<sup>1</sup>; GOLHEN, Stéphane<sup>1</sup>; MIYAZAKI, Akira<sup>2</sup>; ENOKI, Toshiaki<sup>3</sup>; YAMADA, Jun-ichi<sup>4</sup>

(<sup>1</sup>CNRS; <sup>2</sup>Tokyo Inst. Tech.; <sup>3</sup>IMS and Tokyo Inst. Tech.; <sup>4</sup>Univ. Hyogo)

[*C. R. Chim.* **6**, 309–316 (2003)]

The preparation, X-ray crystal structure and magnetic properties of a new charge transfer salt, (DTDH-TTP)Cr(isoq)<sub>2</sub>(NCS)<sub>4</sub>, DTDH-TTP = 2-(1',3'-dithiol-

2'-ylidene)-5-(1'',3''-dithiolan-2''-ylidene)-1,3,4,6-tetrathiapentalene, ISOQ = isoquinoline) are reported. Crystal data: monoclinic, space group  $C2/c$  (#15),  $a = 16.0836(5)$ ,  $b = 19.2488(6)$ ,  $c = 12.6829(6)$  Å,  $\beta = 95.669(1)$ ,  $V = 3906.5(2)$  Å<sup>3</sup>,  $Z = 4$ ,  $R = 0.0515$  for 2899 reflections with  $I > 2\sigma(I)$ . The crystal structure consists of mixed organic and inorganic layers in the  $ac$ -plane, each layer being formed by mixed columns of DTDH-TTP<sup>+</sup> radical cations and paramagnetic metal complex anions. Short intermolecular atomic contacts between donor and anion are observed in the column in the  $c$  direction. Ferrimagnetic interactions are observed between the non-equivalent donor and anion spins. This material exhibits bulk canted weak ferromagnetism below  $T_C = 8.7$  K.

### IV-D-3 Anomalous Metallic State of One-Dimensional Molecular Conductor (EDO-TTFBr<sub>2</sub>)<sub>3</sub>I<sub>3</sub>

MIYAZAKI, Akira<sup>1</sup>; KATO, Takehiko<sup>1</sup>; YAMAZAKI, Hisashi<sup>1</sup>; ENOKI, Toshiaki<sup>2</sup>; OGURA, Eiji<sup>3</sup>; KUWATANI, Yoshiyuki<sup>3</sup>; IYODA, Masahiko<sup>3</sup>; YAMAURA, Jun-ichi<sup>4</sup>

(<sup>1</sup>Tokyo Inst. Tech.; <sup>2</sup>IMS and Tokyo Inst. Tech.; <sup>3</sup>Tokyo Metr. Univ.; <sup>4</sup>Univ. Tokyo)

[*Phys. Rev. B* **68**, 085108 (6 pages) (2003)]

The structure and physical properties of the one-dimensional (1D) molecular conductor (EDO-TTFBr<sub>2</sub>)<sub>3</sub>I<sub>3</sub> are reported. This salt is composed of quasi-1D uniform stacks of the donor molecules and counter anions which are translationally disordered at room temperature. The temperature dependence of the lattice constants shows that, as the temperature decreases, the thermal contraction takes place along the donor columns, leading to the enhancement of the one-dimensionality of the  $\pi$ -electron system. The electrical conductivity and thermoelectric power show a metallic conductivity down to circa 140 K, where a metal-insulator transition takes place. The transition temperature decreases to circa 60 K as the hydrostatic pressure is applied up to 1.1 GPa. Although the transport properties give the itinerant feature of the p-electrons, the static

susceptibility behaves as a 1D Heisenberg antiferromagnet-like behavior of localized spins from room temperature down to 15 K, which is consistent with the ESR linewidth governed by the 1D diffusion mechanism of localized spins. The coexistence of the itinerant character of the transport properties and the localized character of the magnetic properties of the  $\pi$ -electron system is attributed to the strongly correlated nature of the quasi-1D electron system.

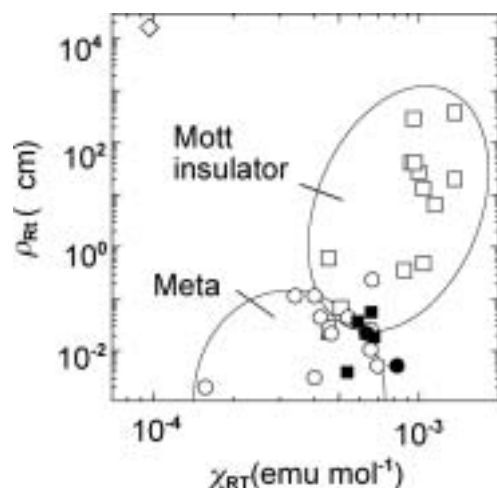


**Figure 1.** The diagram of the resistivities vs. susceptibilities at room temperature for various TTF-based salts. Filled circle: (EDO-TTFBr<sub>2</sub>)<sub>3</sub>I<sub>3</sub>; filled squares: (TMTTF)<sub>2</sub>X; squares: Mott insulators; open circles: metallic compounds; diamond: band insulator.

#### IV-D-4 Property of Self-Assembled Monolayers of Long-Alkyl-Chain-Substituted TTF Derivative

YOKOTA, Yasuyuki<sup>1</sup>; YUGE, Ryota<sup>1</sup>; MIYAZAKI, Akira<sup>1</sup>; ENOKI, Toshiaki<sup>2</sup>; HARA, Masahiko<sup>3</sup>  
(<sup>1</sup>Tokyo Inst. Tech.; <sup>2</sup>IMS and Tokyo Inst. Tech.; <sup>3</sup>RIKEN)

[*Mol. Cryst. Liq. Cryst.* **407**, 121/[517]–127/[523] (2003)]

Self-assembled monolayers (SAMs) of an electron donor TTF derivative with long alkyl chains ( $-\text{C}_{11}\text{H}_{22}-$ ) are formed on Au(111). STM, surface plasmon resonance, and FTIR reflection absorption spectroscopy measurements suggest that TTF backbone is isolated from the gold substrate by long alkyl chains. Cyclic voltammograms reveal two redox peaks ( $E_1^{1/2} = 263$  mV,  $E_2^{1/2} = 508$  mV vs. Ag/Ag<sup>+</sup>) corresponding to TTF/TTF<sup>+</sup> and TTF<sup>+</sup>/TTF<sup>2+</sup>. These peak currents are proportional to the scan rates, indicating that the TTF backbone maintains its electrochemical activity in the SAMs. In addition, the peak-to-peak separations between oxidation and reduction are roughly proportional to the scan rates, which indicates that a potential drop takes place at the long alkyl chains, which work as resistance in the electron transport.

#### IV-D-5 Magnetic Anisotropy of Cerium Endohedral Metallofullerene

INAKUMA, Masayasu<sup>1</sup>; TANIHARA, Atsushi<sup>2</sup>; KATO, Haruhito<sup>2</sup>; SHINOHARA, Hisanori<sup>2</sup>; ENOKI, Toshiaki<sup>3</sup>

(<sup>1</sup>Tokyo Inst. Tech.; <sup>2</sup>Nagoya Univ.; <sup>3</sup>IMS and Tokyo Inst. Tech.)

[*J. Phys. Chem. B* **107**, 6965–6973 (2003)]

Cerium endohedral metallofullerene (Ce@C<sub>82</sub>) is a  $\pi$ - $f$  composite nanomagnet, where anisotropic  $f$ -electron spin is expected to couple with the rotational motion of the fullerene cage that has  $\pi$ -electron spin. The field cooling effect on the susceptibility of Ce@C<sub>82</sub> in organic solutions suggests that the application of a magnetic field forces the molecular orientations to be aligned, in cooperation with the magnetic anisotropy of the  $f$ -electron spin coupled with the molecular orientation. The role of crystal field in the magnetic anisotropy, which is associated with the off-center geometry of the Ce ion in the cage, is clarified by the crystal field analysis. The crystal field effect in the metallofullerene cage is considerably reduced, in contrast to that of ordinary rare-earth compounds. This is consistent with the findings of a small electronic coupling between the  $f$  and  $\pi$ -electrons and a shallow potential of the surrounding cage to the Ce ion. As a consequence, the crystal field effect is emphasized in the low-temperature range (below  $\sim 100$  K).

#### IV-D-6 Resonance Raman Scattering in Carbon Nanotubes and Nanographites

PIMENTA, M. A.<sup>1</sup>; JORIO, A.<sup>1</sup>; DANTAS, M. S.<sup>1</sup>; FANTINI, C.<sup>1</sup>; DE SOUZA, M.<sup>1</sup>; CANÇADO, L. G.<sup>1</sup>; SAMSONIDZE, Ge. G.<sup>2</sup>; DRESSELHAUS, G.<sup>2</sup>; DRESSELHAUS, M. S.<sup>2</sup>; GRÜNEIS, A.<sup>3</sup>; SAITO, Riichiro<sup>3</sup>; SOUZA FILHO, A. G.<sup>4</sup>; KOBAYASHI, Yousuke<sup>5</sup>; TAKAI, Kazuyuki<sup>5</sup>; FUKUI, Ken-ichi<sup>5</sup>; ENOKI, Toshiaki<sup>6</sup>

(<sup>1</sup>Univ. Federal Minas Gerais; <sup>2</sup>MIT; <sup>3</sup>Tohoku Univ., CREST JST; <sup>4</sup>Univ. Federal Ceará; <sup>5</sup>Tokyo Inst. Tech.; <sup>6</sup>IMS and Tokyo Inst. Tech.)

[*Molecular Nanostructures: Proceedings XVII International Winterschool on Electronic Properties of Novel Materials*, H. Kuzmany, J. Fink, M. Mehring and S. Roth, Eds., AIP Conference Proceeding **685**, page 219–224 (2003)]

In this work, we discuss the resonant Raman process in nanographites and carbon nanotubes, relating the most important Raman features to a first-order (single resonance) or a second-order (double resonance) process. We also show that, in the case of 1D systems, the term “resonance” has a more strict meaning and occurs when the energy of the photon does not simply coincide with the energy of a possible electron-hole pair, but rather matches the separation between van Hove singularities in the valence and conduction bands.

#### IV-D-7 Interface Effect on the Electronic Structure of Alkanethiol-Coated Platinum Nanoparticles

TU, Weixia<sup>1</sup>; TAKAI, Kazuyuki<sup>1</sup>; FUKUI, Ken-ichi<sup>1</sup>; MIYAZAKI, Akira<sup>1</sup>; ENOKI, Toshiaki<sup>2</sup>  
(<sup>1</sup>Tokyo Inst. Tech.; <sup>2</sup>IMS and Tokyo Inst. Tech.)

[*J. Phys. Chem. B* **107**, 10134–10140 (2003)]

The structure and electronic properties are investigated for Pt nanoparticles coated with octadecanethiol self-assembled monolayer. The increase in the octadecanethiol/Pt ratio from 0 to full coverage reduces the average particle size from 2.2 to 0.9 nm. The temperature-independent spin susceptibility rises upon the increase in the particle size, quantum size effect being suggested to govern the magnetism. The low-temperature susceptibility shows a large Curie-type divergence, which cannot be explained simply by the even electron state of Pt. XPS spectra suggest an electron deficiency in the interior Pt nanoparticles, which is brought about by charge transfer from nanoparticle to coating thiol monolayer. The ESR line width and the  $g$ -value deviation increase as the octadecanethiol/Pt ratio is elevated, which are associated with the enhancement of spin-orbit interaction at the interface between the interior nanoparticle and coating thiol monolayer. This change at the interface works to make first spin-lattice relaxation centers in the carrier scattering process.

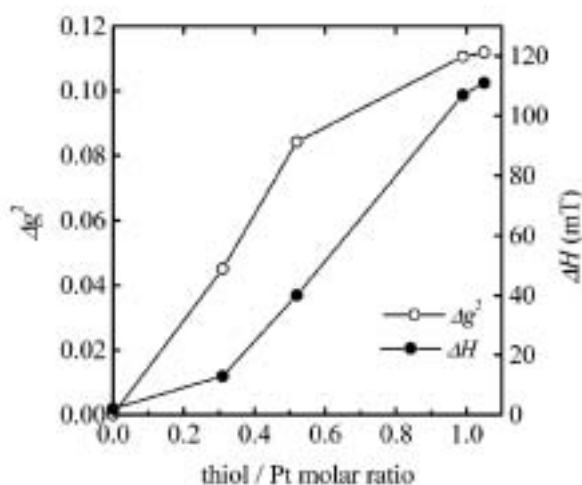


**Figure 1.** The thiol/Pt ratio dependence of  $\Delta g^2$  and  $\Delta H$  measured at room temperature for the thiol-coated Pt nanoparticles. The data for the naked Pt particle (thiol/Pt = 0) is obtained from ref 15.

#### IV-D-8 Tuning Magnetism and Novel Electronic Wave Interference Patterns in Nanographite Materials

HARIGAYA, Kikuo<sup>1</sup>; KOBAYASHI, Yousuke<sup>2</sup>; KAWATSU, Naoki<sup>2</sup>; TAKAI, Kazuyuki<sup>2</sup>; SATO, Hirohiko<sup>3</sup>; RAVIER, Jérôme<sup>2</sup>; ENOKI, Toshiaki<sup>4</sup>; ENDO, Morinobu<sup>5</sup>

(<sup>1</sup>Synthetic Nano-Function Mater. Project, AIST; <sup>2</sup>Tokyo Inst. Tech.; <sup>3</sup>Chuo Univ.; <sup>4</sup>IMS and Tokyo Inst. Tech.; <sup>5</sup>Shinshu Univ.)

[*Physica E* **22**, 708–711 (2004)]

Antiferromagnetism in stacked nanographite is investigated with using the Hubbard-type models. The A–B stacking or the stacking near to that of A–B type is favorable for the hexagonal nanographite with zigzag edges, in order that magnetism appears. We also find that the open shell electronic structure can be an origin of the decreasing magnetic moment with the decrease of the inter-graphene distance, as experiments on adsorption of molecules suggest. Next, superperiodic patterns with a long distance in a nanographene sheet observed by STM are discussed in terms of the interference of electronic wave functions. The period and the amplitude of the oscillations decrease spatially in one direction. We explain the superperiodic patterns with a static linear potential theoretically. In the  $k$ - $p$  model, the oscillation period decreases, and agrees with experiments. The spatial difference of the static potential is estimated as 1 : 3 eV for 200 nm in distance, and this value seems to be reasonable in order that the potential difference remains against perturbations, for example, by phonon fluctuations and impurity scatterings. It turns out that the long-distance oscillations come from the electronic structure of the two-dimensional graphene sheet.

#### IV-D-9 Magnetic Phase Diagram of Three-Dimensional Diluted Ising Antiferromagnet Ni<sub>0.8</sub>Mg<sub>0.2</sub>(OH)<sub>2</sub>

SUZUKI, Masatsugu<sup>1</sup>; SUZUKI, Itsuko<sup>1</sup>; ONYANGO, Tedamann M.<sup>1</sup>; ENOKI, Toshiaki<sup>2</sup>  
(<sup>1</sup>State Univ. New York Binghamton; <sup>2</sup>IMS and Tokyo Inst. Tech.)

[*J. Phys. Soc. Jpn.* **73**, 206–215 (2004)]

$H$ - $T$  diagram of 3D diluted Ising antiferromagnet Ni <sub>$c$</sub> Mg<sub>1- $c$</sub> (OH)<sub>2</sub> with  $c = 0.8$  has been determined from measurements of SQUID DC magnetization and AC magnetic susceptibility. At  $H = 0$ , this compound undergoes two magnetic phase transitions: an antiferromagnetic (AF) transition at the Néel temperature  $T_N$  (= 20.7 K) and a reentrant spin glass (RSG) transition at  $T_{RSG}$  ( $\approx 6$  K). The  $H$ - $T$  diagram consists of the RSG, spin glass (SG), and AF phases. These phases meet a multicritical point  $P_m$  ( $H_m = 42$  kOe,  $T_m = 5.6$  K). The irreversibility of susceptibility defined by  $\delta$  ( $= \chi_{FC} - \chi_{ZFC}$ ) shows a negative local minimum for  $10 \leq H \leq 35$  kOe, suggesting the existence of possible glassy phase in the AF phase. A broad peak in  $\delta$  and  $\chi''$  at  $H \geq 20$  kOe for  $T_N(c = 0.8, H) \leq T \leq T_N(c = 1, H = 0)$  (= 26.4 K) suggests the existence of the Griffiths phase.

#### IV-D-10 STM Observation of Electronic Wave Interference Effect in Finite-Sized Graphite with Distortion-Network Structures

KOBAYASHI, Yousuke<sup>1</sup>; TAKAI, Kazuyuki<sup>1</sup>; FUKUI, Ken-ichi<sup>1</sup>; ENOKI, Toshiaki<sup>2</sup>; HARIGAYA, Kikuo<sup>3</sup>; KABURAGI, Yutaka<sup>4</sup>; HISHIYAMA, Yoshihiro<sup>4</sup>

(<sup>1</sup>Tokyo Inst. Tech.; <sup>2</sup>IMS and Tokyo Inst. Tech.; <sup>3</sup>Synthetic Nano-Function Mater. Project, AIST;

<sup>4</sup>Musashi Inst. Tech.)

[*Phys. Rev. B* **69**, 035418 (7 pages) (2004)]

Superperiodic patterns near a step edge were observed by scanning tunneling microscopy on several-layer-thick graphite sheets on a highly oriented pyrolytic graphite substrate, where a dislocation network is generated at the interface between the graphite overlayer and the substrate. Triangular- and rhombic-shaped periodic patterns whose periodicities are around 100 nm were observed on the upper terrace near the step edge. In contrast, only outlines of the patterns similar to those on the upper terrace were observed on the lower terrace. On the upper terrace, their geometrical patterns gradually disappeared and became similar to those on the lower terrace without any changes of their periodicity in increasing a bias voltage. By assuming a periodic scattering potential at the interface due to dislocations, the varying corrugation amplitudes of the patterns can be understood as changes in the local density of states as a result of the beat of perturbed and unperturbed waves, *i.e.*, the interference in an overlayer. The observed changes in the image depending on an overlayer height and a bias voltage can be explained by the electronic wave interference in the ultrathin overlayer distorted under the influence of dislocation-network structures.

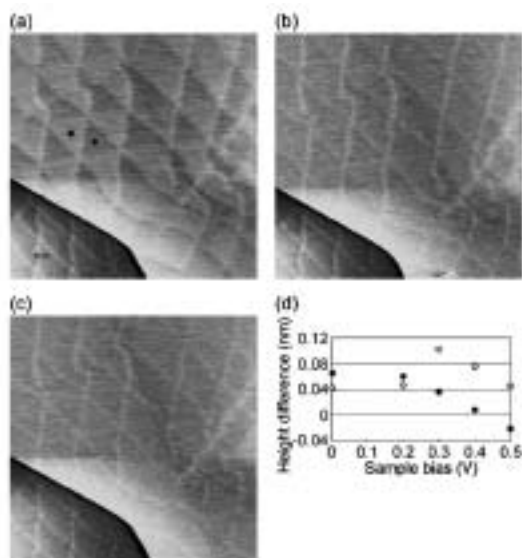


**Figure 1.** STM images ( $500 \times 500 \text{ nm}^2$ ) of superperiodic patterns at higher sample bias voltages; (a)  $V_s = 0.3 \text{ V}$ , (b)  $V_s = 0.4 \text{ V}$ , and (c)  $V_s = 0.5 \text{ V}$ . By increasing the bias voltage, the corrugation amplitude of superperiodic patterns on the upper terrace decreased gradually [(a) and (b)] and changed into a net pattern (c). In contrast, no significant change was observed for the pattern on the lower terrace. The net pattern appearing on the upper terrace of (c) is similar to that on the lower terrace. Height differences between two points depicted in (a) are shown in (d) for clarifying the bias-dependent contrast. Solid and blank circles are the height differences of the upper and lower terrace, respectively. (Circles at the sample bias of around 0 V are the height differences at  $V_s = 0.02 \text{ V}$ .)

#### IV-D-11 STM Observation of the Quantum Interference Effect in Finite-Sized Graphite

KOBAYASHI, Yousuke<sup>1</sup>; TAKAI, Kazuki<sup>1</sup>; FUKUI, Ken-ichi<sup>1</sup>; ENOKI, Toshiaki<sup>2</sup>; HARIGAYA, Kikuo<sup>3</sup>; KABURAGI, Yutaka<sup>4</sup>; HISHIYAMA, Yukihiro<sup>4</sup>  
 (<sup>1</sup>Tokyo Inst. Tech.; <sup>2</sup>IMS and Tokyo Inst. Tech.; <sup>3</sup>Synthetic Nano-Function Mater. Project, AIST; <sup>4</sup>Musashi Inst. Tech.)

[*J. Phys. Chem. Solids* **65**, 199–203 (2004)]

Superperiodic patterns were observed by STM on two kinds of finite-sized graphene sheets. One is nanographene sheets inclined from a highly oriented pyrolytic graphite (HOPG) substrate and the other is a several-layer-thick graphene sheets with dislocation-network structures against a HOPG substrate. As for the former, the in-plane periodicity increased gradually in the direction of inclination, and it is easily changed by attachment of a nanographite flake on the nanographene sheets. The oscillation pattern can be explained by the interference of electron waves confined in the inclined nanographene sheets. As for the latter, patterns and their corrugation amplitudes depended on the bias voltage and on the terrace height from the HOPG substrate. The interference effect by the perturbed and unperturbed waves in the overlayer is responsible for the patterns whose local density of states varies in space.

#### IV-D-12 Theoretical Study on Novel Electronic Properties in Nanographite Materials

HARIGAYA, Kikuo<sup>1</sup>; YAMASHIRO, Atsushi<sup>2</sup>; SHIOMI, Yukihiro<sup>1</sup>; WAKABAYASHI, Katsunori<sup>3</sup>; KOBAYASHI, Yousuke<sup>4</sup>; KAWATSU, Naoki<sup>4</sup>; SATO, Hirohiko<sup>5</sup>; RAVIER, Jérôme<sup>4</sup>; ENOKI, Toshiaki<sup>6</sup>; ENDO, Morinobu<sup>7</sup>  
 (<sup>1</sup>Synthetic Nano-Function Mater. Project, AIST; <sup>2</sup>AIST; <sup>3</sup>Hiroshima Univ.; <sup>4</sup>Tokyo Inst. Tech.; <sup>5</sup>Chuo Univ.; <sup>6</sup>IMS and Tokyo Inst. Tech.; <sup>7</sup>Shinshu Univ.)

[*J. Phys. Chem. Solids* **65**, 123–126 (2004)]

Antiferromagnetism in stacked nanographite is investigated with using the Hubbard-type model. We find that the open shell electronic structure can be an origin of the decreasing magnetic moment with the decrease of the inter-layer distance, as experiments on adsorption of molecules suggest. Next, possible charge-separated states are considered using the extended Hubbard model with nearest-neighbor repulsive interactions. The charge-polarized state could appear, when a static electric field is present in the graphene plane for example. Finally, superperiodic patterns with a long distance in a nanographene sheet observed by STM are discussed in terms of the interference of electronic wave functions with a static linear potential theoretically. In the analysis by the  $k$ - $p$  model, the oscillation period decreases spatially in agreement with experiments.

#### IV-D-13 Structure and Physical Properties of Molecular Magnets Based on Transition Metal Complexes of Crown Thioether

**NISHIJO, Junichi<sup>1</sup>; MIYAZAKI, Akira<sup>1</sup>; ENOKI, Toshiaki<sup>2</sup>**

(<sup>1</sup>Tokyo Inst. Tech.; <sup>2</sup>IMS and Tokyo Inst. Tech.)

[*Bull. Chem. Soc. Jpn.* **77**, 715–727 (2004)]

A new series of molecule-based magnets, including crown thioether (9S3 = 1,4,7-trithiacyclononane) complexes of transition metals (Ni, Co, Cu), are presented. TCNQ salts [M(9S3)<sub>2</sub>](TCNQ)<sub>2</sub> (M = Ni, Co) are one-dimensional (1D), antiferromagnetic (AF) complexes with an intra-chain interaction  $J = -3.9$  K and  $-1.3$  K for M = Ni and Co, respectively, despite its long intermolecular distance, for which the large spin density on the sulfur atom in the magnetic [M(9S3)<sub>2</sub>]<sup>2+</sup> cation is responsible. The mixed valence salt [M(9S3)<sub>2</sub>](TCNQ)<sub>3</sub> (M = Ni, Co) is a paramagnetic semiconductor. 1D AF magnet [Cu(9S3)Br<sub>2</sub>] does not undergo any magnetic transition because of the weak inter-chain interaction. Substituting a very small amount (~ 5%) of Cu with Ni causes a structural change. The change decreases the distances of inter-chain S–S contacts, resulting in the generation of an AF transition at  $T_N = 4.5$  K. [M(9S3)<sub>2</sub>][Ni(bdt)<sub>2</sub>]<sub>2</sub> (M = Ni, Co; bdt = 1,2-benzenedithiolato) are weak-ferromagnets with  $T_N = 6.2$  K and 2.6 K for M = Ni and Co, respectively. In the crystals, [M(9S3)<sub>2</sub>]<sup>2+</sup>–[Ni(bdt)<sub>2</sub>]<sup>–</sup> alternate chains and [Ni(bdt)<sub>2</sub>]<sup>–</sup> uniform chains coexist. The appearance of weak-ferromagnetism is associated with a competition between two kinds of inter-chain AF interactions between [M(9S3)<sub>2</sub>]<sup>2+</sup>–[Ni(bdt)<sub>2</sub>]<sup>–</sup> alternate chains, where the stronger one is an indirect inter-chain interaction through [Ni(bdt)<sub>2</sub>]<sup>–</sup> uniform chains, while the weaker is a direct inter-chain interaction.

#### IV-D-14 Effect of Heat-Treatment on Magnetic Properties of Non-Graphitic Disordered Carbon

**TAKAI, Kazuyuki<sup>1</sup>; OGA, Meigo<sup>1</sup>; ENOKI, Toshiaki<sup>2</sup>; TAOMOTO, Akira<sup>3</sup>**

(<sup>1</sup>Tokyo Inst. Tech.; <sup>2</sup>IMS and Tokyo Inst. Tech.;

<sup>3</sup>Matsushita Electric Industrial Co., Ltd.)

[*Diamnod Rel. Mater.* **13**, 1469–1473 (2004)]

Heat-treatment effect on the electronic properties is investigated by magnetic susceptibility and ESR measurements in relation to structural change for non-graphitic but sp-rich disordered carbon thin-film prepared by pulsed laser deposition. X-ray 2 diffraction reveals that the sp<sup>2</sup> sp<sup>3</sup>-jumbling “non-graphitic” structure of non-heat-treated sample with atomic-scale disorder is easily relaxed into the nano-sized “graphitic” island-network by heat-treatment at approximately 600 °C, preserving the sp<sup>2</sup>/sp<sup>3</sup> ratio in the sample at ~90%. According to the temperature dependence of magnetic susceptibility, non-heat-treated sample shows the Curie-Weiss behavior with the large Pauli paramagnetic temperature-independent term and antiferromagnetic interaction whose strength is significantly larger than that simply expected from the average spin–spin distance. The temperature dependence of ESR signal intensity confirms the large contribution of the Pauli paramagnetism in the non-heat-treated sample.

#### IV-D-15 Development of TTF-Based Self-Assembled Monolayer Systems and Their Electronic Properties

**ENOKI, Toshiaki<sup>1</sup>; YOKOTA, Yasuyuki<sup>2</sup>; YUGE, Ryota<sup>2</sup>; TU, Weixia<sup>2</sup>; MIYAZAKI, Akira<sup>2</sup>; TAKAI, Kazuyuki<sup>2</sup>; FUKUI, Ken-ichi<sup>2</sup>**

(<sup>1</sup>IMS and Tokyo Inst. Tech.; <sup>2</sup>Tokyo Inst. Tech.)

[*J. Phys. IV France* **114**, 667–671 (2004)]

Self-assembled monolayer (SAM) systems of alkanethiol and TTF-substituted alkanethiol molecules on Au substrate and metal nanoparticles are investigated. TTF-substituted alkanethiol molecules form charge transfer complex SAM with TCNQ molecules, where charge transfer (CT) rate becomes similar to that in bulk TTF-TCNQ crystal. TTF-substituted alkanethiol SAMs with long alkyl chains shows Coulomb-blockade-type electron transport owing to the resistance of the long alkyl chain bridge. In Pt nanoparticles with alkanethiol SAMs on their surface, CT takes place from core Pt nanoparticle to surface SAMs, producing an electron deficient state in Pt core nanoparticle. Pd nanoparticles with SAMs of mixtures of alkanethiol and TTF-substituted alkanethiol molecules take a large reduction of the Pauli paramagnetic susceptibility, which is brought about by CT.

#### IV-D-16 Crystal Structure and Physical Properties of (EDO-TTFBr<sub>2</sub>)<sub>2</sub>FeX<sub>4</sub> (X = Cl, Br)

**MIYAZAKI, Akira<sup>1</sup>; AIMATSU, Masashi<sup>1</sup>; YAMAZAKI, Hisashi<sup>1</sup>; ENOKI, Toshiaki<sup>2</sup>; UGAWA, Kouhei<sup>3</sup>; OGURA, Eiji<sup>3</sup>; KUWATANI, Yoshiyuki<sup>3</sup>; IYODA, Masahiko<sup>3</sup>**

(<sup>1</sup>Tokyo Inst. Tech.; <sup>2</sup>IMS and Tokyo Inst. Tech.; <sup>3</sup>Tokyo Metropolitan Univ.)

[*J. Phys. IV France* **114**, 545–547 (2004)]

The crystal structure and physical properties of radical ion salts (EDO-TTFBr<sub>2</sub>)<sub>2</sub>FeX<sub>4</sub> (X = Cl, Br) composed of halogen-substituted organic donor and magnetic halide anions are investigated. The salts consist of uniformly stacked donor molecules, whose Br substituents are connected to halide ligands of anions with remarkably short intermolecular contacts. Both salts show metallic behavior above ca. 30 K. The FeCl<sub>4</sub> salt shows an antiferromagnetic (AF) transition at  $T_N = 4.2$  K despite the absence of anion···anion contacts, thus the magnetic interaction between the localized spins on the anions is mediated by the  $\pi$ - $d$  interaction through the Br···Cl contacts. For the FeBr<sub>4</sub> salt the AF transition temperature is elevated to  $T_N = 13.5$  K, accompanied with another anomaly at  $T_{C2} = 8.5$  K. This behavior can be qualitatively explained by a magnetic structure model where the  $\pi$ - $d$  interaction between donor and anion is taken into account.

#### IV-D-17 Strong $\pi$ - $d$ Interaction Based on Brominated TTF-Type Donor EDT-TTFBr<sub>2</sub>

**NISHIJO, Junichi<sup>1</sup>; MIYAZAKI, Akira<sup>1</sup>; ENOKI,**

Toshiaki<sup>2</sup>; WATANABE, Ryoji<sup>2</sup>; KUWATANI, Yoshiyuki<sup>3</sup>; IYODA, Masahiko<sup>3</sup>  
 (<sup>1</sup>Tokyo Inst. Tech.; <sup>2</sup>IMS and Tokyo Inst. Tech.; <sup>3</sup>Tokyo Metropolitan Univ.)

[*J. Phys. IV France* **114**, 561–563 (2004)]

New  $\pi$ - $d$  interacting system based on brominated TTF-type donor EDT-TTFBr<sub>2</sub> (= 4,5-dibromo-4',5'-ethylenedithiotetrathiafulvalene) was investigated. Magnetic (EDT-TTFBr<sub>2</sub>)<sub>2</sub>FeBr<sub>4</sub> and non-magnetic (EDT-TTFBr<sub>2</sub>)<sub>2</sub>GaBr<sub>4</sub> are isostructural salts, which have strong anion-donor interaction through Br–Br atomic contacts with weak direct anion-anion interaction. The iron salt takes an antiferromagnetic transition at  $T_N = 11$  K owing to strong  $\pi$ - $d$  interaction, which originates from the strong anion-donor interaction. The strong  $\pi$ - $d$  interaction also plays an important role in the electron transport phenomenon in the variation of temperature and applied magnetic field.

#### IV-D-18 Anisotropy of the Raman Spectra of Nanographite Ribbons

CANÇADO, L. G.<sup>1</sup>; PIMENTA, M. A.<sup>1</sup>; NEVES, B. R. A.<sup>1</sup>; MEDEIROS-RIBEIRO, G.<sup>2</sup>; ENOKI, Toshiaki<sup>3</sup>; KOBAYASHI, Yousuke<sup>4</sup>; TAKAI, Kazuyuki<sup>4</sup>; FUKUI, Ken-ichi<sup>4</sup>; DRESSELHAUS, M. S.<sup>5</sup>; SAITO, Riichiro<sup>6</sup>; JORIO, A.<sup>1</sup>

(<sup>1</sup>Univ. Federal Minas Gerais; <sup>2</sup>Laboratório Nacional Luz Sincrotrão; <sup>3</sup>IMS and Tokyo Inst. Tech.; <sup>4</sup>Tokyo Inst. Tech.; <sup>5</sup>MIT; <sup>6</sup>Tohoku Univ. and CREST JST)

[*Phys. Rev. Lett.* **93**, 047403 (4 pages) (2004)]

A polarized Raman study of nanographite ribbons on a highly oriented pyrolytic graphite substrate is reported. The Raman peak of the nanographite ribbons exhibits an intensity dependence on the light polarization direction relative to the nanographite ribbon axis. This result is due to the quantum confinement of the electrons in the 1D band structure of the nanographite ribbons, combined with the anisotropy of the light absorption in 2D graphite, in agreement with theoretical predictions.

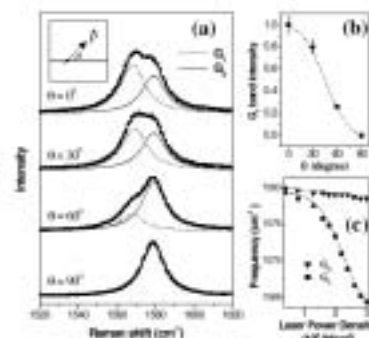


**Figure 1.** (a) Raman spectra obtained for light incident with different polarization angles ( $\theta$ ) with respect to the ribbon direction. The inset shows a schematic figure of the sample (horizontal gray line) showing the direction between the ribbon axis and the light polarization vector ( $\vec{P}$ ). (b) Intensity of the  $G_1$  peak versus  $\theta$ . The dotted line is a  $\cos 2\theta$  theoretical curve. The error bars are associated with baseline corrections. (c) Raman frequencies of the  $G_2$  (triangles) and  $G_1$  (squares) peaks as a function of the laser power density.